Supplementary Material

The fate of arsenic in groundwater discharged to the Meghna River, Bangladesh

Michelle Berube,[A] Katrina Jewell,[B] Kimberly D. Myers,[C] Peter S. K. Knappett,[C,F] Pin Shuai,[C] Abrar Hossain,[D] Mehtaz Lipsi,[D] Sadam Hossain,[D] Alamgir Hossain,[D] Jacqueline Aitkenhead-Peterson,[E] Kazi M. Ahmed[D] and Saugata Datta[A]

[A]Department of Geological Sciences, 108 Thompson Hall, Kansas State University, Manhattan, KS 66506, USA.
[B]Water Management and Hydrologic Sciences Program, 611 Ross Street, Texas A&M University, College Station, TX 77845, USA.
[C]Department Geology and Geophysics, Texas A&M University, College Station, TX 77845, USA.
[D]Department Geology, University of Dhaka, Dhaka 1000, Bangladesh.
[E]Department Soil and Crop Science, Texas A&M University, College Station, TX 77845, USA.
[F]Corresponding author. Email: knappett@tamu.edu

Supplemental Videos

Video S1. Tidal fluctuations in a riverbank aquifer in the dry season along the Meghna River (January 12-16, 2015). The blue grad symbol represents the Meghna River level. The orange grad symbols with distance from the river are the monitoring wells T6, T5, Veast1a and T1. All wells are screened at the same depth 16 m below land surface at T1. The cause of the fluctuations are semi-diurnal tides in the Bay of Bengal. https://youtu.be/pseu80g0Gx8

Video S2. Tidal fluctuations in a riverbank aquifer in the dry season along the Meghna River under the influence of nearby irrigation pumping. The blue grad symbol represents the Meghna River level. The orange grad symbols with distance from the river are the monitoring wells T6, T5, Veast1a and T1. All wells are screened at the same depth 16 m below land surface at T1. The cause of the fluctuations are semi-diurnal tides in the Bay of Bengal. https://youtu.be/QqMpNMd8OV4

Table S1. Field analyte test kits and a list of standard methods associated, purchased in December, 2015 for the January, 2016 field season from CHEMetrics, Inc. (Midland, VA). Precision is indicated by the number of decimal places included in the analytical range, and additional information regarding each method is available at the company website (www.chemetrics.com).

Analyte	Range (ppm)	Method	CHEMetrics, Inc. Method ID
Dissolved Oxygen (DO)	0-1.000	Rhodazine D	K-7553
Dissolved Oxygen (DO)	0-15.0	Indigo Carmine	K-7513
Dissolved Oxygen (DO)	0-1.0	Rhodazine D	K-7501
Nitrate (as NO_3^-)	0-50.0	Cadmium Reduction	K-6933
Ammonia (NH_3)	0-30.0	Salicylate	K-1403
Ortho-phosphate (PO_4^{3-})	0-1.0; 1-10	Stannous Chloride	K-8510
Sulfate (SO_4^{2-})	0-100.0	Turbidimetric	K-9203
Soluble manganese (Mn)	0-30.0	Periodate	K-6503
Total and Ferrous Iron (Fe(II), Fe)	0-6.00	Phenanthroline	K-6203
Total and Soluble Iron (Fe)	0-25.0	Phenanthroline	K-6013
Total Iron	0-30.0; 30-300	Phenanthroline	K-6210D
Sulfide (H_2S/HS^-)	0-6.00	Methylene Blue	K-9523
Sulfide	0-1.0; 1-10	Methylene Blue	K-9510

Table S2. Model parameters input for the flow and transport model

Parameters	Units	Value
Hydraulic conductivity (K)	md^{-1}	22.5
Effective Porosity	-	0.35
Residual Water Content	-	0.1
van Genuchten (α)	m^{-1}	10
van Genuchten (n)	-	2
Longitudinal dispersivity	m	1
Transversal dispersivity	m	0.1
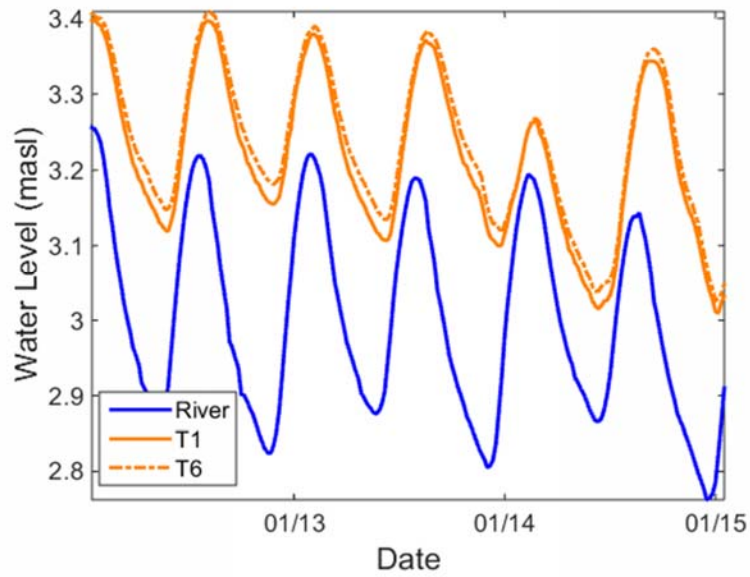
Figure S1. Hydrographs of tidal fluctuations in a riverbank aquifer in the dry season along the Meghna River (January 12-15, 2015). All wells are screened at the same depth 16 m below land surface at T1.
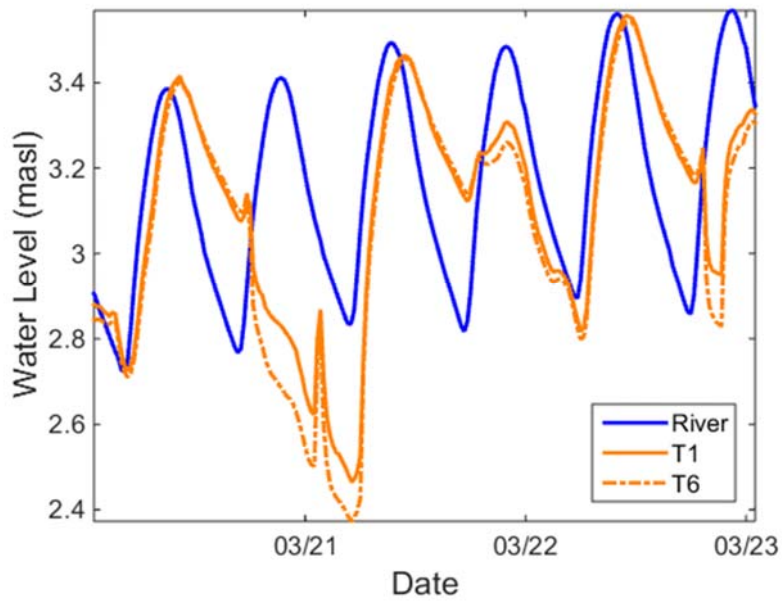
Figure S2. Hydrographs of tidal fluctuations in a riverbank aquifer in the dry season along the Meghna River under the influence of irrigation pumping (March 20-23, 2015). All wells are screened at the same depth 16 m below land surface at T1.
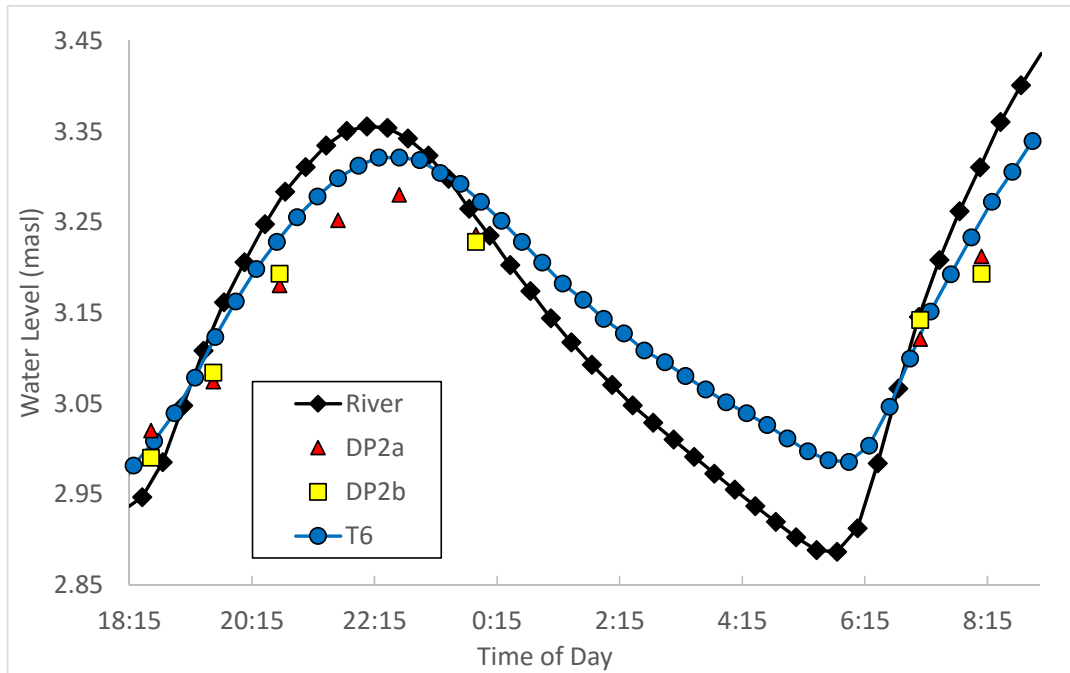
Figure S3. Observed vertical hydraulic heads below the seepage face over one semi-diurnal (12 hour) tidal cycle (January 11-12, 2016). The crest of the peak represents losing conditions for the river, whereas the troughs represent gaining conditions where groundwater flows towards the river.
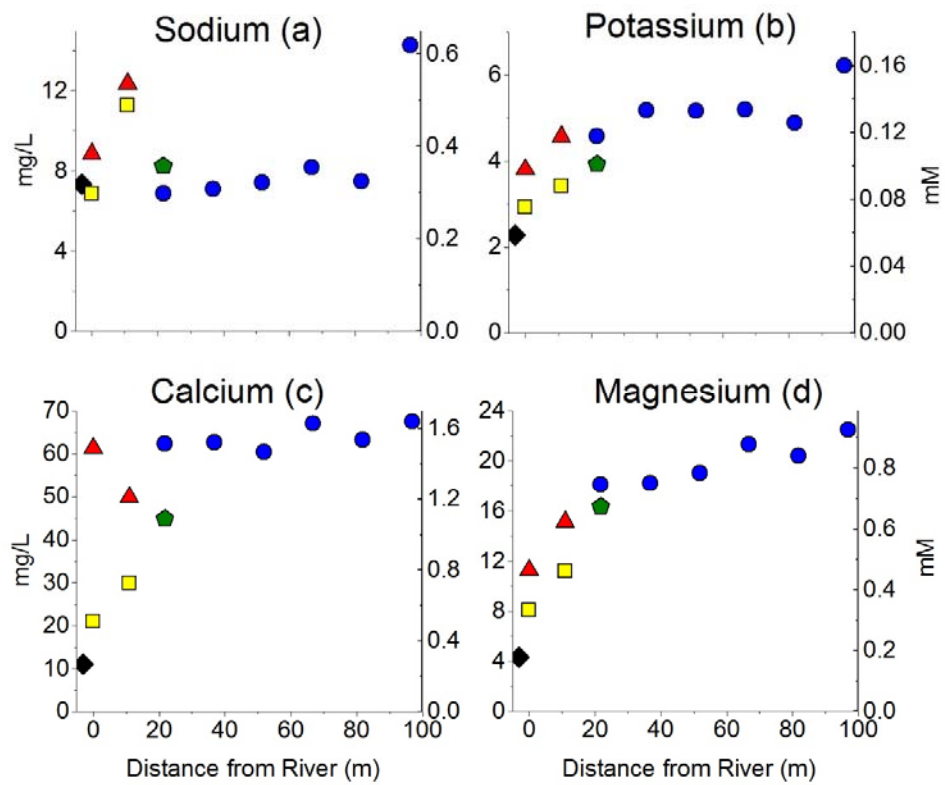
Figure S4. Major cation concentrations across the riverbank aquifer (Veast). Blue circles and green pentagons designate 16 and 7 m deep monitoring wells respectively. Yellow squares and red triangles designate 3 and 1 m depth drive-point piezometers, respectively. Black diamonds designate the river water. The distance from the river was measured during the low river stage in January.
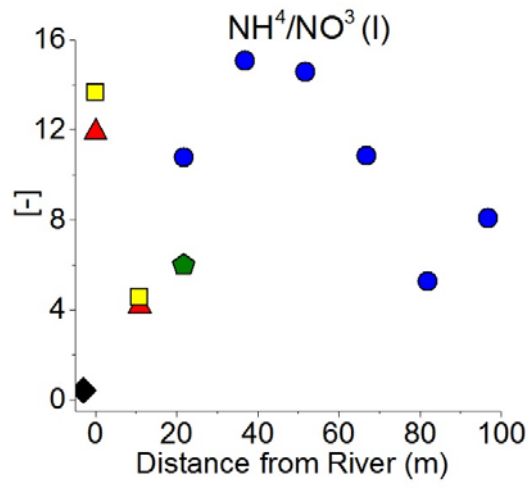
Figure S5. Molar ammonium to nitrate ratio across the Veast monitoring well transect.
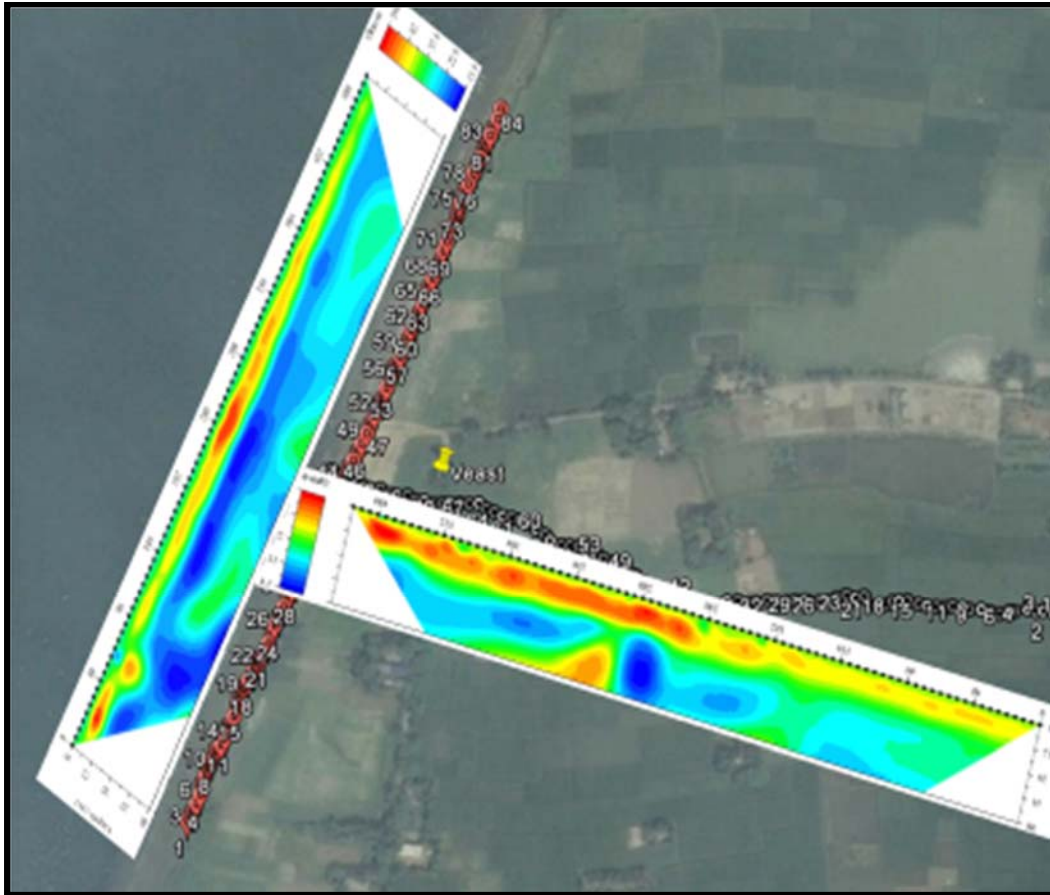
Figure S6. ERT profiles demonstrating the continuity of the shallow 25 m thick aquifer 581 m inland and along the river's edge. Red colors indicate highly resistive sand (60-100 mS/m), and dark blue and green indicate electrically conductive silt or clay layers (10-40 mS/m). The T1 well at the Veast site is indicated by the yellow thumbtack.
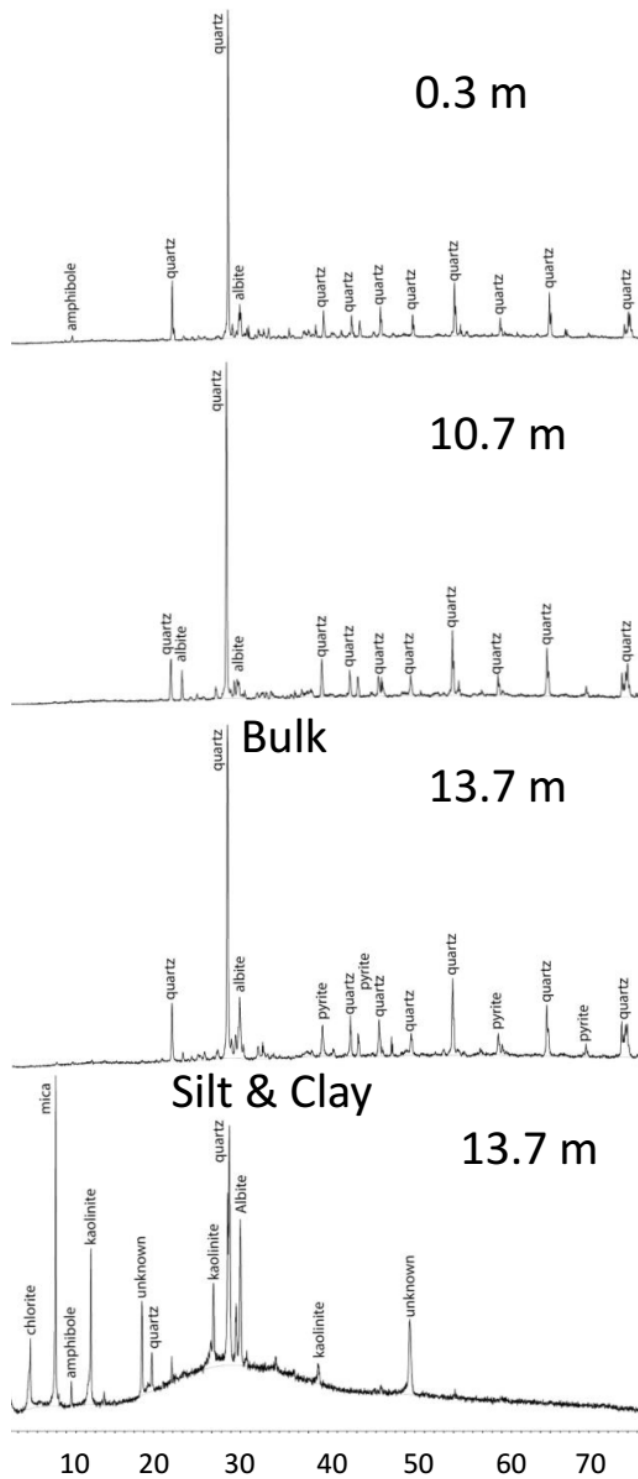
Figure S7. Mineralogical analysis on borehole cuttings from T7 using X-ray Diffraction. The x-axis units are 2 theta and the y-axis is counts. The sample at 13.7 m was analyzed in bulk and only silt and clay.
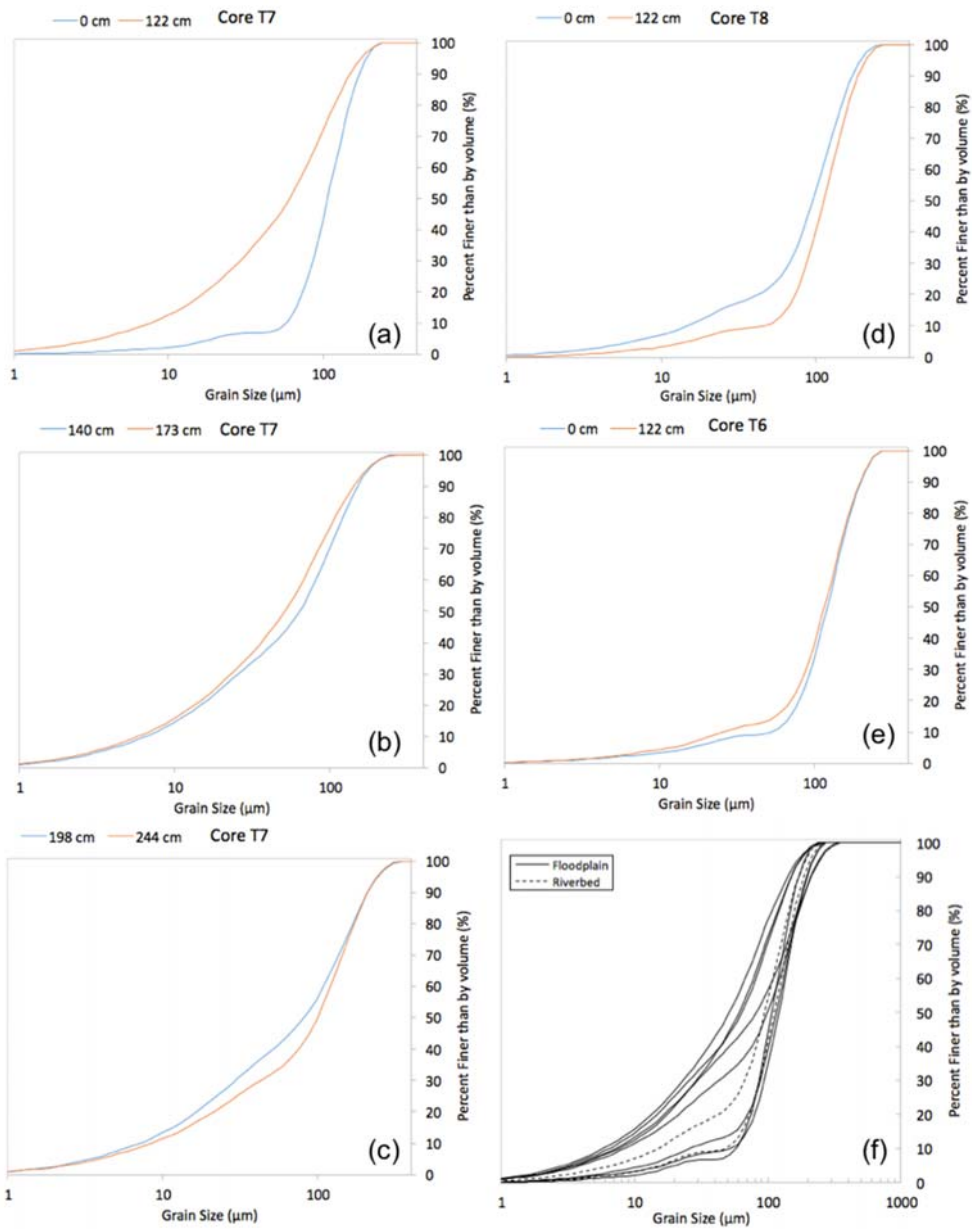
Figure S8. Grain size analysis for Core T7 (a, b, c) Core T8 (d) and Core T6 (e) and Comparison of Grain sizes for the sediment along the floodplain verses on the riverbed (f).
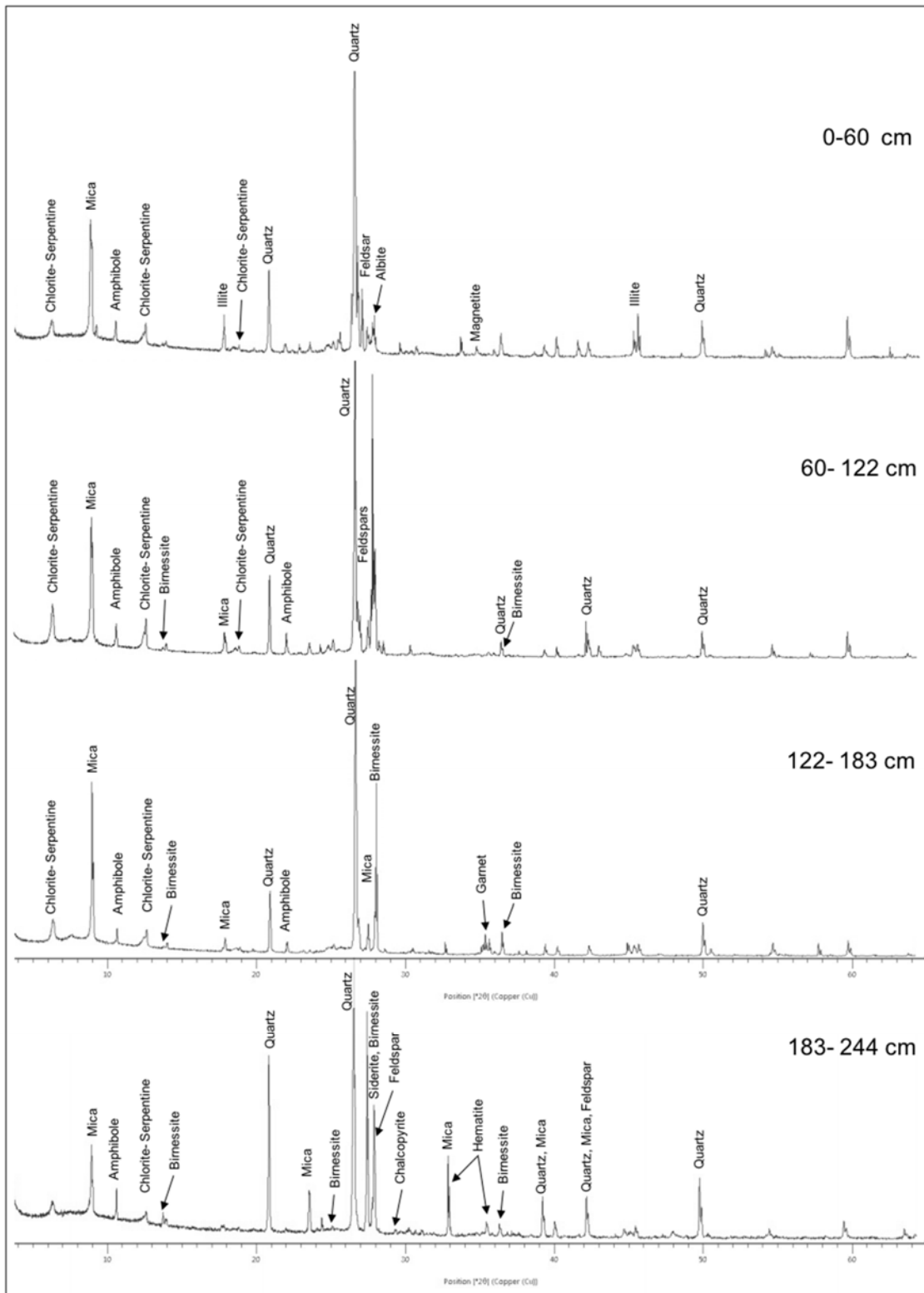
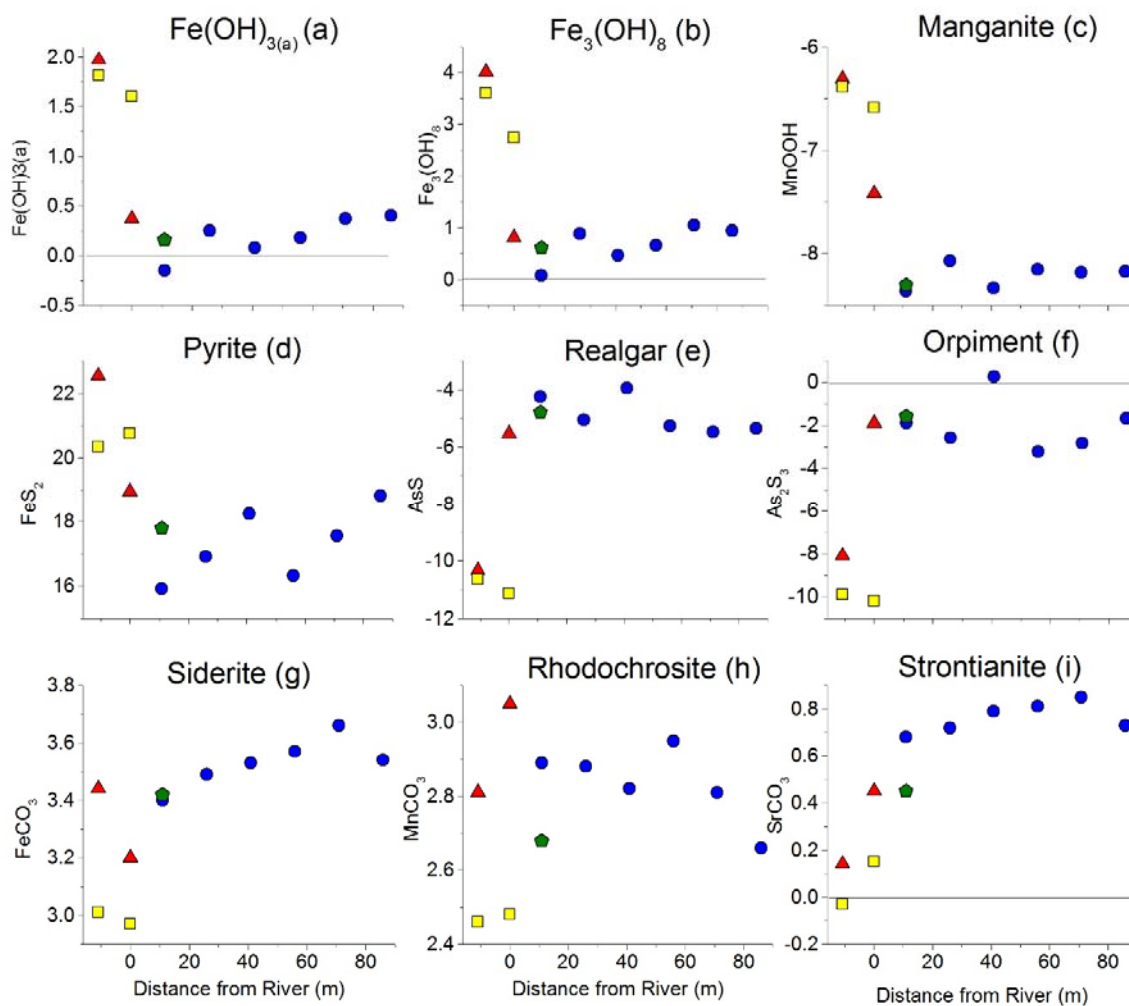Figure S9. Mineral assemblage for Core T7 by X-Ray Diffraction

Figure S10. Saturation Indices along riverbank aquifer flow pathway. Blue circles and green pentagons designate 16 and 7 m deep monitoring wells respectively. Yellow squares and red triangles designate 3 and 1 m depth drive-point piezometers, respectively.
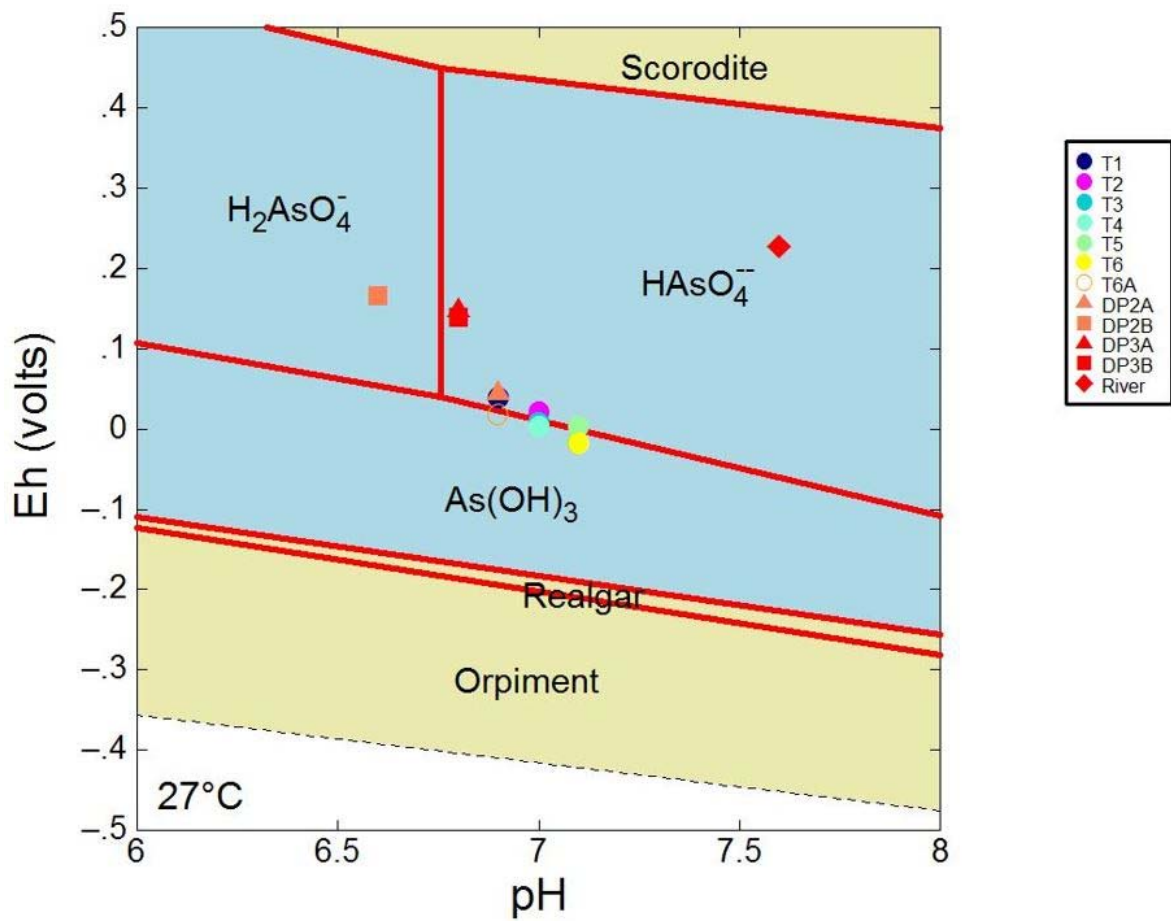
Figure S11. Diagram As(OH)$_4$, T = 27°C, P = 1.013 bars, a[main] = 10^{-6}, a[H$_2$O] = 1, a[Fe^{2+}] = 10^{-4}, a[HCO$_3$] = 1, a[SO$_4^{2-}$] = 10^{-5} This model shows each well and drive point piezometer graphed with respect to their measured pH and Eh values. The graph is on top of a phase diagram which shows the expected phases of arsenic, iron, sulfate, and bicarbonate at the Eh-pH range at our study site. The warmer colors are closest to the river. This figure shows what compounds and their phases, dissolved (blue) or precipitated (orange) could be in the water in each well and drive point piezometer. These results indicate that the hyperheic or the shallow groundwater aquifer zones aren't reduced enough environments to precipitate As-sulfur minerals such as realgar and orpiment.
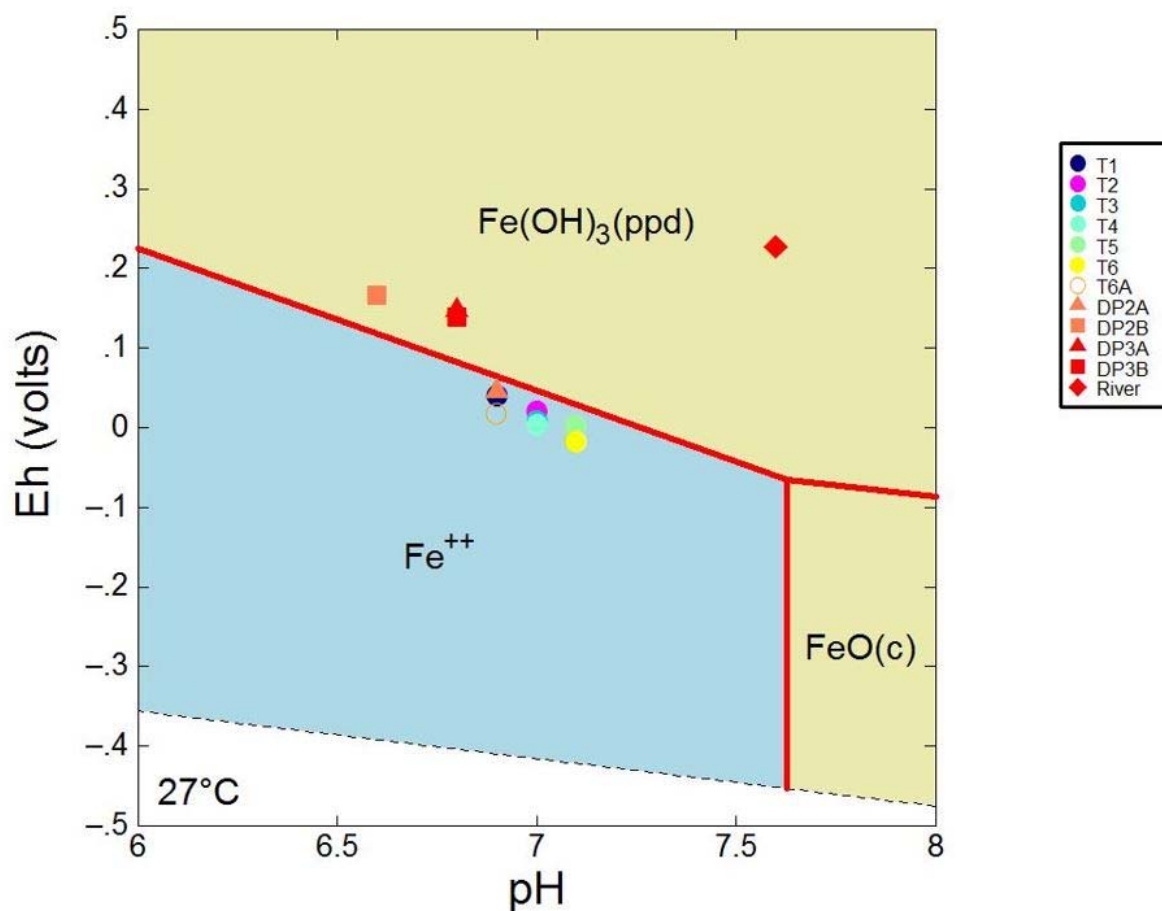
Figure S12. Diagram Fe^{2+}, T = 27°C, P = 1.013 bars, a[main] = 10^{-4}, a[H$_2$O] = 1; Suppressed: Goethite, Hematite, Magnetite. This model shows each well and drive point piezometer graphed with respect to their measured pH and Eh values. The graph is on top of a phase diagram which shows the expected phases of only iron at the Eh-pH range at our study site. The warmer colors are closest to the river. The minerals hematite, goethite, and magnetite were not considered in the model since there would be too little time at our site for them to precipitate. This model shows what dissolved (blue) and precipitated (blue) iron phases could be occurring at each well and drive point piezometer. The results indicate that some wells will contain primarily aqueous Fe(II) in solution or precipitated Fe oxides.